J Fluoresc (2006) 16:793–807
DOI 10.1007/s10895-006-0123-7

ORIGINAL PAPER

Ruby Crystal for Demonstrating Time- and Frequency-Domain Methods of Fluorescence Lifetime Measurements

Danielle E. Chandler · Zigurts K. Majumdar · Gregor J. Heiss · Robert M. Clegg

Received: 12 June 2006 / Accepted: 9 August 2006 / Published online: 22 September 2006

Abstract We present experiments that are convenient and educational for measuring fluorescence lifetimes with both time- and frequency-domain methods. The sample is ruby crystal, which has a lifetime of about 3.5 milliseconds, and is easy to use as a class-room demonstration. The experiments and methods of data analysis are used in the lab section of a class on optical spectroscopy, where we go through the theory and applications of fluorescence. Because the fluorescence decay time of ruby is in the millisecond region, the instrumentation for this experiment can be constructed easily and inexpensively compared to the nanosecond-resolved instrumentation required for most fluorescent compounds, which have nanosecond fluorescence lifetimes. The methods are applicable to other luminescent compounds with decay constants from microseconds and longer, such as transition metal and lanthanide complexes and phosphorescent samples. The experiments, which clearly demonstrate the theory and methods of measuring temporally resolved fluorescence, are instructive and demonstrate what the students have learned in the lectures without the distraction of highly sophisticated instrumentation.

Keywords Fluorescence · Luminescence · Lifetimes · Time-domain · Frequency-domain · Phosphorescence · Ruby · Phase · Modulation · Lockin

Introduction

The growing importance of fluorescence lifetime imaging in biology and medicine, along with the increase in instrumental sophistication [1–3], presents the challenge of effectively teaching these techniques and the physics behind them to students, and to other practicing researchers. In the last few years we have created a course on "optical spectroscopy" in the Physics Department at the University of Illinois, Urbana-Champaign. The course consists of three hours of theoretical lectures per week and a three hour weekly laboratory section. The material covered in the laboratory section is extensive. Because the theoretical lectures explore mostly the fundamental physics of optical spectroscopy, the laboratory sections are critical practical extensions to the lectures, and are to a great extent self-contained. This is a graduate course (open also to advanced undergraduates), and is attended by students from physics, engineering, chemistry, and biophysics.

One of the major laboratory topics is a hands-on practical introduction to luminescence lifetimes, and we introduce both time- and frequency-domain technologies [1, 4]. Because the normal fluorescence experiments typically involve nano- or pico-second lifetimes and modulation frequencies of hundreds of megahertz in the frequency-domain, the instrumentation for measuring rapid fluorescence decay is both expensive and relatively complex compared to the instrumentation usually available in an educational laboratory class [5, 6]. Although we also introduce the sophisticated instrumentation for measuring nanosecond fluorescence time decays in the time-domain [1] and frequency-domain (including both the heterodyne and homodyne methods [4]), and give demonstrations of the techniques on existing professional instrumentation, the complexity of the nanosecond time-resolved (photon counting time-resolved techniques [1]) and high frequency instrumentation [4, 6] makes it difficult for the students to carry out hands-on experimentation, where they can participate in planning and carrying out the assembly of the instrumentation. In addition, the measurement

D. E. Chandler · Z. K. Majumdar · G. J. Heiss · R. M. Clegg (✉)
Physics Department, University of Illinois Urbana-Champaign,
1110 West Green Street, Urbana, IL 61801
e-mail: rclegg@uiuc.edu

of very high frequency signals requires heterodyne or homodyne technology for reducing the frequency of the measured signal to much lower frequencies, more convenient for data acquisition. These techniques, common in radio electronics [7] and the electronics of lock-in amplifiers [8–10], introduce unnecessary complications, and make it more difficult for the students to concentrate on the spectroscopic phenomenon and the basics of frequency-domain measurements. In order for the students to focus on the fundamental aspects of practical time-resolved spectroscopy measurements without worrying about sophisticated photon counting techniques and high frequency electronics, and to construct affordable and relatively simple instrumentation suitable for a class environment, we have developed the classroom laboratory instrumentation and exercise described in this report.

The experiments take advantage of the unusually long fluorescence lifetime of solid ruby [11–15]. The millisecond-range lifetime of ruby permits the use of hertz-kilohertz-range light modulation, and the fluorescence signal can be handled directly with normal low frequency computer data acquisition and common lock-in amplifiers [8, 9, 16, 17]. The optical instrumentation and electronic circuits can be set up by the students themselves. The fluorescence lifetime of ruby, which is temperature-dependent [15, 18] is also of some intrinsic interest as a thermometer.

In this report, we concentrate on the emission from ruby crystals because ruby is a very convenient sample with no sample preparation and no decomposition; however, there are many other slowly emitting chromophores that are suitable if one wishes to include different samples, or emphasize certain applications. The long lifetimes of certain luminophores (in the microsecond to second time range) is often due to phosphorescence decay of organic chromophores. Phosphorescence is the slow emission from the triplet state following intersystem crossing from the initially excited singlet state to the triplet state [19, 20]. Slow emission, in the microsecond to second time range, has been used in many applications, such as studying rotational diffusion of proteins in membranes [21, 22] and oxygen sensing [23–25]. Long-lived luminescent compounds have also been used as probes of pressure on solid surfaces [26]. The very slow emission from Terbium and Europium ions (chelated in a complex with organic chromophores) are used extensively for spectroscopic assays for following pH changes and halide concentrations [27], as well as for time-resolved imaging [28] and assay [29] applications.

Experimental setup

Two setups for this luminescence lifetime spectroscopy experiment are discussed; they differ in the source of the modulated excitation light and the mode of data collection.

Set-up 1

In the first setup (Fig. 1) the light from a Hg-Xe arc lamp is focused onto the chopper blade of a variable-speed beam chopper (Ithaco, Ithaca, HMS Light Beam Chopper 221, Chopper Head 220A). It is important to focus the excitation light onto the chopper blade to a small spot to minimize the on-off transient flanks of the repetitive excitation. The excitation light is then collimated with another lens, passed through a 390-nm excitation filter, and finally focused onto the sample. The luminescence is collected and collimated into a parallel beam with a single lens, passed through a high pass 600-nm emission filter, and finally focused onto the detector. Figure 1 is a block diagram of the general setup.

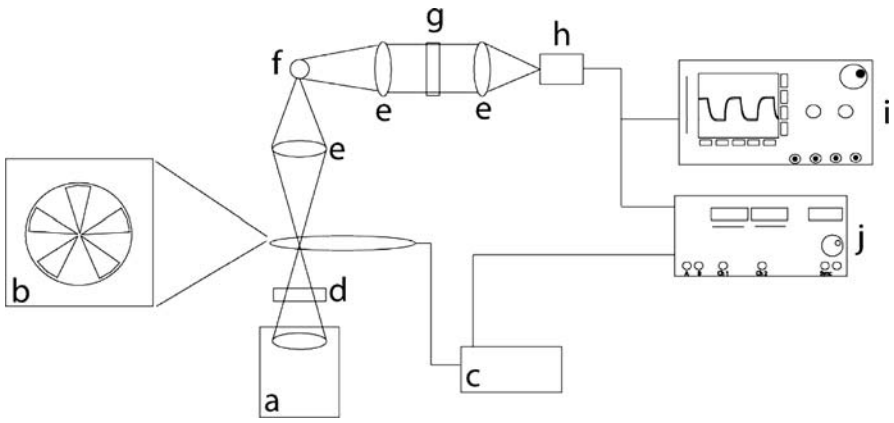

Fig. 1 A block diagram of Setup 1. Light from a Xe-Hg arc lamp (a) is directed through a 390-nm excitation filter (d) and focused onto the ruby or rhodamine sample (f) with a lens (e). The excitation light is modulated with a beam chopper (b) and a variable-speed chopper controller (c). The fluorescence light from the sample is passed through a 600-nm emission filter (g) and onto the detector (h). Data from the detector may be collected using an oscilloscope (i) or lock-in amplifier (j)

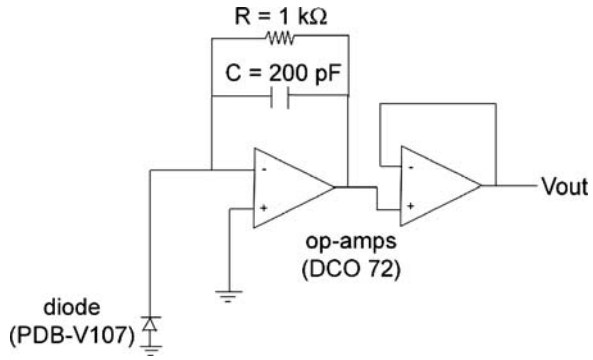

Fig. 2 The detector used in this experiment is constructed of a photodiode (model PDB-V107) and a current-to-voltage converter consisting of a 1 kΩ resistor, a 200 pF capacitor and two op-amps (model DCO 72). This inexpensive detector is simple enough to be constructed by students

The detector in Fig. 1 is a solid-state photodiode (model PDB-V107), which produces a current proportional to the intensity of the incident light. A current-to-voltage converter transforms the current from the photodiode into a usable output voltage signal. A schematic of this current-to-voltage converter circuit is shown in Fig. 2. The output of the detector can be sent to an oscilloscope, lock-in amplifier or computer data acquisition card, which can then be analyzed by any convenient software (such as Excel, LabView or Igor). This setup can be used for both time-domain and frequency-domain lifetime measurements.

Set-up 2

The second experimental setup is shown in Fig. 3, and will be discussed in detail below.

Some of the experiments with the equipment of Fig. 3 were carried out with the arc lamp (or LED in continuous mode) and chopper replaced with a 370-nm laser diode (LED) that is directly modulated with either the analog output of a National Instruments DAQ card, or an amplified audio source from a PC (Fig. 3). The LED can be modulated up to sufficiently high frequencies with an arbitrary waveform.

Samples

Two fluorescent samples are used for the experiments: ruby and rhodamine. The organic fluorophore serves as a reference; convenient reference fluorophores are rhodamine B, tetramethyl-rhodamine or rhodamine 6G, all which are readily available and have fluorescence lifetimes from 1.5 to 4 nanoseconds. The exact lifetime of the rapid decay of the organic fluorophore is not important. The nanosecond decay of the organic fluorophores is six orders of magnitude faster that the ruby (essentially instantaneous relative to the

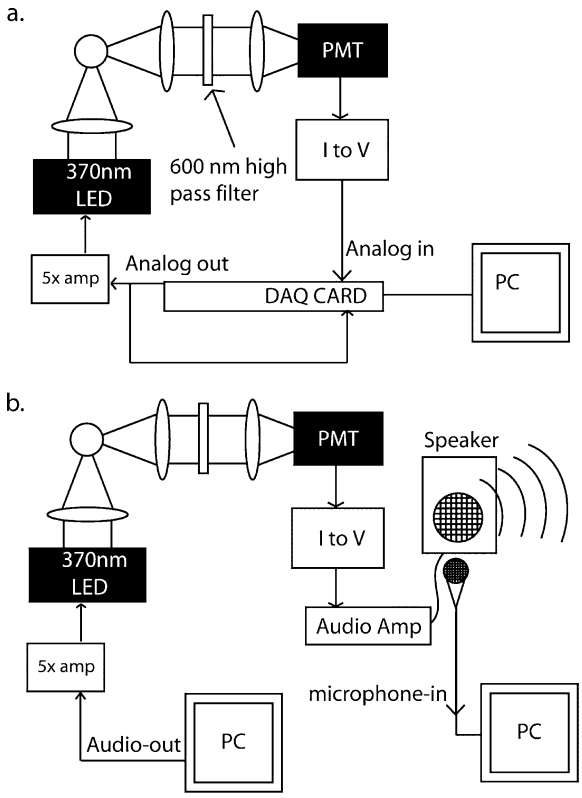

Fig. 3 Experimental schematic for diode modulation and acquisition with a data acquisition, DAQ, card. (a) An arbitrary analog signal is generated from the card using LabView, sent through a 5× amplifier to modulate the intensity of the diode about a DC offset. The PMT collects the ruby emission and the signal from the current to voltage converted is collected by the DAQ card at the appropriate sampling rate. (b) Similar to a, but the diode is modulated with an audio output from a PC playing an mp3 file. The voltage from the PMT is sent through an audio amplified to a speaker, which can be heard and recorded with a microphone into a standard music file (e.g., .mp3 or .WAV) and can then be analyzed

ruby decay), and is used for calibrating the time course of the modulated excitation light. The sample, a clear single crystal ruby, (purchased from International Monocrystal Corporation, 2596 Elgro Road, Gibsonia, PA) has an emission lifetime of about 3–4 ms. Both the rhodamine and ruby samples can be excited with 390-nm light and they fluoresce in the 600-nm range. Similar results can be achieved with raw natural ruby available from many places on the web; but these samples are usually not as bright.

Solid ruby makes an excellent specimen for this luminescence lifetime experiment for several reasons. It has a very long fluorescence lifetime of approximately 3.7 ms, and its photophysics is well-known because of its use in the pulsed ruby laser. Additionally, the use of ruby is convenient because it can be stored easily and indefinitely for future use (unlike more volatile fluorescent solutions), and because quality synthetic ruby is quite inexpensive. Figure 4 shows the dominant time-dependent radiative process in ruby; its

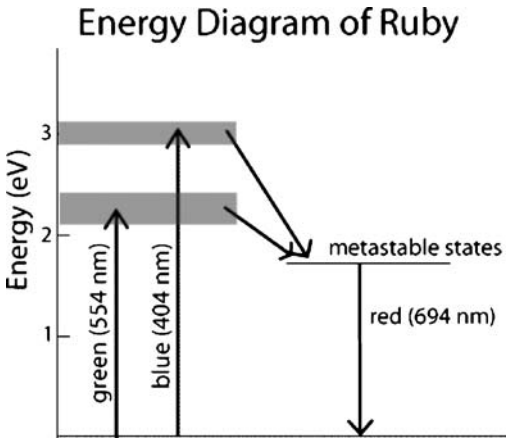

Fig. 4 The energy diagram of the major transitions of ruby is shown. The fluorescence lifetime at 0.05% Cr_2O_3 is about 3 ms at 300 K. The fluorescence line width at 300 K is 5.0 Angstroms. The major absorption bands are at 404 nm and 554 nm, and the fluorescence is at 694.3 nm

lifetime is temperature-dependent [18]. The chromium impurities absorb light in the green and blue regions. The initially populated excited states relax to a meta-stable state before eventually dropping back to the ground state, giving off the familiar 694-nm red light of ruby emission [30, 31].

Usually an extremely high energy is required to excite paired electrons in most inorganic substances, resulting in electronic absorptions in the ultraviolet. However, when unpaired electrons are present in transition-metal compounds, usually in d or f orbitals, then the absorptions can occur at lower energies. This leads to the ligand-field colors and provides the colors of many minerals and paint pigments. The transition metal may be only an impurity (<1%). This provides the color in many of gemstones.

A pure Corundum crystal (pure Al_2O_3) is sapphire. In this colorless material each aluminum ion is surrounded by six oxygens in a distorted octahedron. All electrons are paired. Replacing approximately 0.5–1% aluminums by a chromium (creating ruby) leads to absorption and luminescence. Chromium in the trivalent state has 18 paired electrons in the *1s* through *3p* orbitals, and three unpaired electrons in the *3d* orbitals. The initial excitation is to energy levels that are broad due to the effect of the surrounding Al_2O_3 crystal structure (this is advantageous for laser action, because a broad spectrum of excitation light can be used to excite the ruby). These initial excited levels decay very rapidly to the intermediate metastable state (much faster than non-radiative transitions to the ground state). The metastable state has a very narrow energy level, because the electrons in this state, active in the transition, are well protected from the environment. The transition to the ground state from this metastable state is long (3 ms), as is expected from the energy-time uncertainty principle (narrow energy transition corresponds to longer lifetimes).

Data analysis

The data acquisition and analysis demonstrate two different experimental determinations of luminescence lifetimes: time-domain and frequency-domain measurements. The time-domain measurement records directly the exponentially-decaying luminescence response. Since ruby has such a long fluorescence lifetime, the exponential rise and fall of the response to a square wave excitation can be seen easily on an oscilloscope. As shown below for both modes of data acquisition (time- and frequency-domain), the quantitative models are straight forward, and if time is available the programs can be written by the students as part of the exercise. Alternatively, the experimenter can also read the approximate 1/e values of the time decays off the display of an analog oscilloscope (Figs. 1 and 3a), or when exciting with a sinusoidal modulation with the LED (Fig. 3a) the phase delay and demodulation of the ruby compared to the rhodamine sample can also be read approximately from the oscilloscope traces. This visual display is impressively educational; the students can easily see the basic, raw fluorescence data before they are operated on by any software. Examples are given below.

Convolution of the fluorescence response with the excitation wave form

The response of the fluorescence system is identical to any linear, damped oscillation system that is driven by a repetitive forcing function. In general, the response to an arbitrary excitation function $E(t)$ is just the convolution of $E(t)$ and $F_\delta(t)$:

$$F(t) = Q \int_0^t E(t')F_\delta(t - t')dt'. \quad (1)$$

$F(t)$ is the measured fluorescence signal, $F_\delta(t)$ is the normalized fluorescence response to a delta pulse of excitation, and Q is a materials- and instrumental-dependent constant. For a single fluorescent component, $F_\delta(t)$ is a exponential decay; for multiple components, $F_\delta(t)$ is a weighted sum of exponential decays. In order to determine the fluorescence lifetime (which we assume here to be from a single fluorescence component) the fluorescence signal must be deconvoluted from the form of the excitation light $E(t')$. This is true for a direct time-domain experiment, as well as for the frequency-domain. To take into account that the repetitive

excitation modulation may not be a pure sine curve, $E(t')$ is written in terms of its complex Fourier expansion.[1]

$$F(t) = Q \int_0^t \left[\sum_{n=-N}^{N} E_n e^{i\omega_n t'} \right] A e^{-(t-t')/\tau} dt'. \qquad (2)$$

N is the maximum number of independent Fourier frequency components describing the excitation waveform, A is the amplitude of the fluorescence species with lifetime τ, and $\omega_n = n\omega_0$. Students wishing to review the theory of Fourier expansions could refer to common references [7, 32–35]. Equations 1 and 2 simply say that the fluorescence response at time t to a short excitation pulse (delta function) at time t' is proportional to $e^{-(t-t')/\tau}$ (causality), and all excitation time-increments are summed over all Fourier components of the repetitive excitation waveform. Equation 2 emphasizes the close relationship of the time- and frequency-domain measurements. In both cases, Equation 2 is the starting point for describing the signal.

Time-domain

The time-domain measurement is easy to understand. The luminescence response to a delta-function excitation pulse of a single fluorescent species is a simple exponential decay: $F_\delta = Ae^{-t/\tau}$ [20]. A is the recorded amplitude and τ is the fluorescence lifetime. If the excitation pulse is not very short compared to the fluorescence lifetime, then the recorded signal must be deconvoluted from the shape of the excitation pulse in order to recover the pure exponential decay (see Equation 1). If the excitation light is modulated as a square wave, during the "light on" phase the fluorescence signal increases as $A_{\text{on}}(1 - e^{-(t-t^0_{i,\text{on}}/\tau)})$, and during the "light off" phase the fluorescence decreases exponentially as $A_{\text{off}}e^{-(t-t^0_{i,\text{off}}/\tau)}$ [28]. After several periods of oscillation, the signal reaches a steady state, the amplitudes become time independent, and $A_{\text{on}} = A_{\text{off}}$. $t^0_{i,\text{on}}$ and $t^0_{i,\text{off}}$ are the times that ith the excitation square wave excitation is turned on or off. The measurement is made during this steady state, averaging many cycles of the excitation waveform [28].

Frequency domain

The frequency-domain measurement is understood best by assuming that the excitation light varies as a simple sinusoid. If the excitation is not a pure sine wave, it can be decomposed into a series of sinusoids by Fourier analysis, Equation 2.The idea behind the frequency-domain measurement is that the luminescence signal suffers a frequency-dependent demodulation (decreasing depth of modulation of the fluorescence signal compared to the modulation depth of the excitation light) and a phase shift (delay) relative to the excitation light due to the finite luminescence time constant of the fluorescent sample. The theory behind this effect is presented in many references [1, 2, 4–6, 19], but some aspects are repeated here for clarity and completeness.

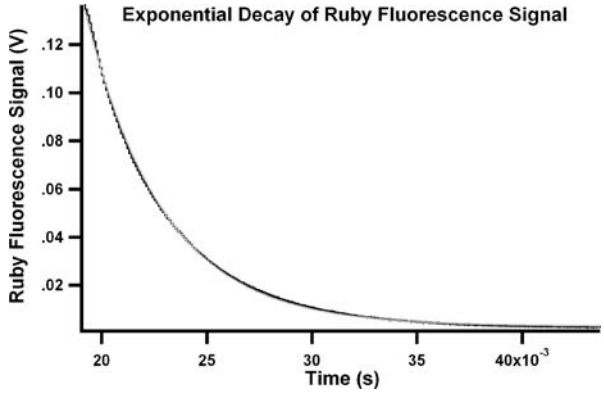

Fig. 5 A digital reference output from the chopper controller, synchronous with the pulse repetition frequency, is used to trigger the oscilloscope for synchronous data acquisition. After acquiring the data with the digital oscilloscope, the data were transferred to a computer (the data could also be acquired directly in a computer with a DAQ card, as depicted in Fig. 3). The data are transferred to a spread sheet and the regression analysis is carried out with any convenient fitting program. The data are fitted to a single exponential decay, giving a lifetime of 3.71 ms with a χ^2 value of 0.00379. The fit is shown in light grey over the data, which is displayed in black

Sinusoidal excitation and a single fluorescence lifetime component

For a simple sine wave excitation of the form

$$E(t) = E_0 + 2E_1 \cos(\omega t) = E_0 + E_1(e^{i\omega t} + e^{-i\omega t}), \qquad (3)$$

and for a single relaxing fluorescence component, the fluorescence response reduces to

$$\begin{aligned} F(t) &= F_0 + F_1(\omega)\cos(\omega t + \phi) \\ &= Q \int_0^t (E_0 + 2E_1 \cos(\omega t)) A e^{-(t-t')/\tau} dt' \\ &= Q \left[E_0 A\tau + E_1 \left(\frac{2A\tau}{\sqrt{1+(\omega t)^2}} \cos(\omega\tau + \tan^{-1}(\omega\tau)) \right) \right] \\ &= QA\tau[E_0 + 2ME_1 \cos(\omega\tau + \phi)] \end{aligned} \qquad (4)$$

[1] Any repetitive function can be expanded in a Fourier series. The expression for this series expansion can be expressed either in real form $y(t) = A_0/2 + \sum_{m=1}^{\infty}(A_m \cos m\omega_0 t + B_m \sin m\omega_0 t)$, or complex form: $y(t) = \sum_{m=-\infty}^{\infty} C_m \exp(im\omega_0 t)$. ω_0 is the fundamental frequency (the period is $T = 2\pi/\omega_0$), m is an integer. $1/2A_0$, A_m and B_m are the DC-offset and the mth sine and cosine component amplitudes, and $C_m = (A_m^2 + B_m^2)^{1/2}$.

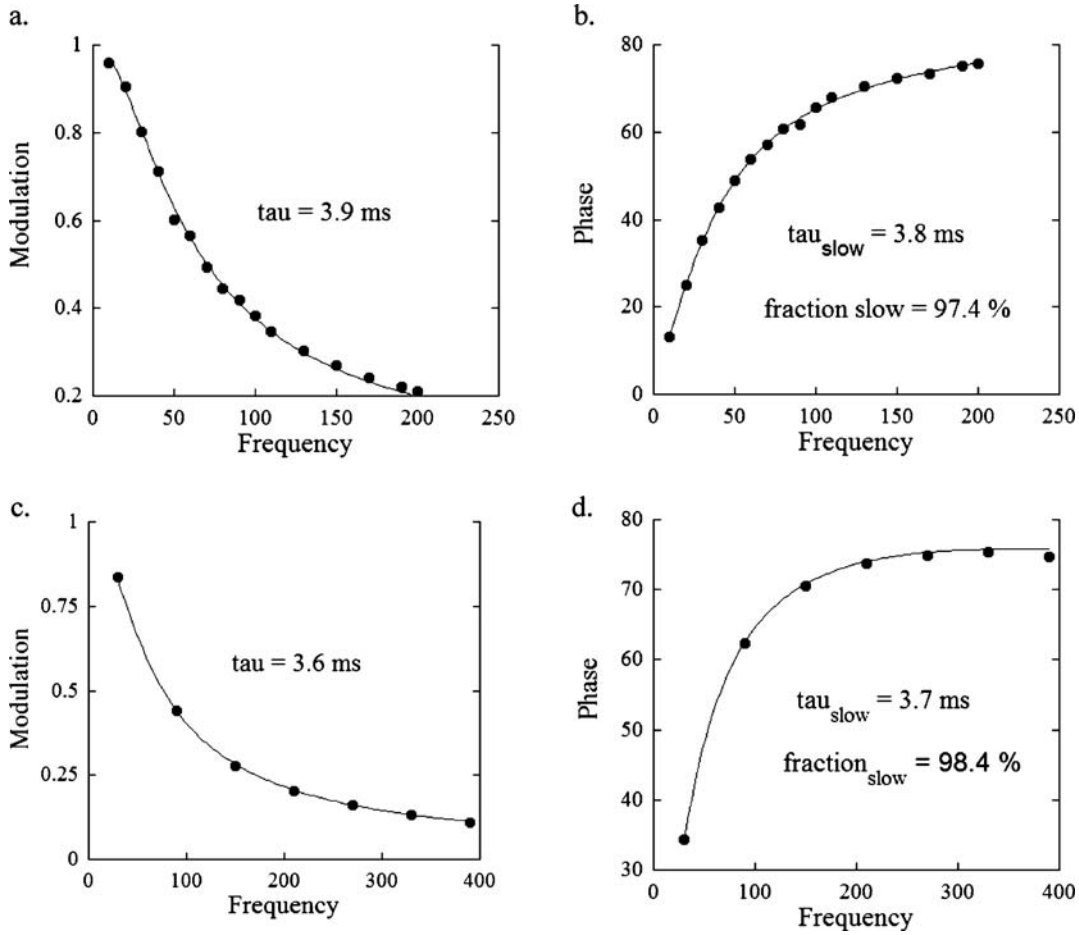

Fig. 6 Modulation, a and c, and phase, b and d, vs. frequency of experiment carried out with square wave modulation of the excitation light. The data in a and c are fit to the expression for modulation of a single component, Equation 5. The phase data of b and d are fit to an expression for two components, see Footnote 3. See the text for the explanation why we cannot observe the minor, very fast second component in the modulation data. Note, although the minor component is less that a few %, it is easily seen at the higher frequencies in the phase data. See the text for discussion

In Equation 4,

$$M = \frac{F_1(\omega)/F_0}{E_1/E_0} = \frac{1}{\sqrt{1+(\omega\tau)^2}} \tag{5}$$

and

$$\phi = \tan^{-1}(\omega\tau) \tag{6}$$

are the demodulation and phase shift of the luminescence signal relative to the excitation light. As the frequency increases, the modulation depth decreases toward zero and the phase increases to a maximum of $\pi/2$. By measuring the modulation depth and the phase at many frequencies, the lifetime can be determined. Two independent estimates are determined, τ_M from Equation 5, and τ_ϕ from Equation 6.

Square wave excitation for the frequency domain

When the arc lamp or the LED in continuous mode and beam chopper are used, the excitation light is not a simple sine wave, but a repetitive square wave. Any repetitive function can be expanded in a Fourier series (see Footnote 1). There are an infinite number of Fourier frequency components in the Fourier expansion of a square wave.[2] Due to the finite lifetime, the signal of fluorescence is not a square wave but is a repetitive signal with exponentially increasing and decreasing flanks. It can also be expressed as a Fourier expansion. The analysis in the last section can be applied to

[2] The Fourier expansion of a pure square wave of period T and minimum and maximum amplitude 0 and A is $y(t)_{\text{Sq Wave}} = A/2 + 2A/\pi \sum_{\substack{m=\text{odd} \\ \text{positive intergers}}} \frac{1}{m} \sin\left(\frac{m2\pi t}{T}\right)$

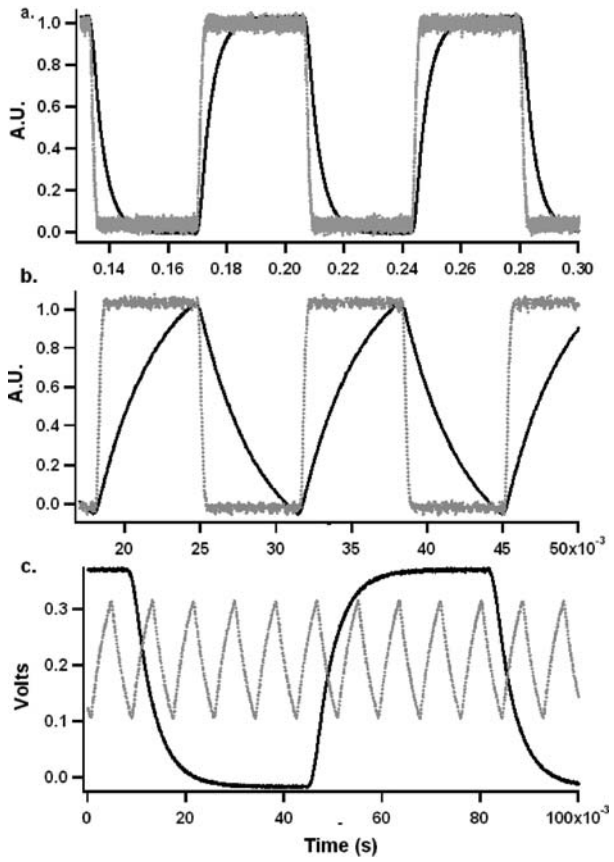

Fig. 7 Square wave modulation of rhodamine and ruby with a chopper. For **a**) and **b**), ruby in solid lines (black) and rhodamine in dotted lines (grey) **a**) 13.6 Hz, **b**) 74 Hz. **c**) comparison of ruby modulation at 13.6 (solid black) and 120 Hz (dotted grey). Shown in **c**) is the symmetry of the time constant for the rise and decrease in intensity as a result of square wave modulation. **c**) shows also the decrease in modulation with increased frequency

each frequency component of the Fourier expansion of both the excitation (rhodamine signal) and fluorescence signal (ruby signal); each component of the expansion is independent of all others. In particular, the fundamental frequency component is of primary interest in this paper. However, we mention that one can analyze the higher frequency components of the signal resulting from a repetitive square-wave excitation, by either carrying out a digital Fourier analysis of a digitally recorded time record of the signal or using a lock-in amplifier (see next paragraph) in a mode that is sensitive to the higher harmonics of the repetition frequency. A frequency dispersion curve of the demodulation extent and phase delay can be acquired to determine more than a single lifetime (see Fig. 6d, and the corresponding text). One can also determine the frequency dispersion curve by carrying out the experiment at different fundamental frequencies of the beam chopper, and analyzing the fundamental frequency component at each frequency (see Figs. 6a, b, and Fig. 7).

Synchronous detection with a lock-in or digital computer data acquisition

If such a repetitive signal is analyzed using a lock-in amplifier, the lock-in can be set to select only the fundamental frequency component of the signal (many introductory references to lock-in amplifiers can be found in the literature [8–10, 16, 17, 36]). A lock-in is essentially a frequency filter with an extremely narrow bandwidth. This very narrow bandwidth is achieved by the synchronous detection of the signal with a reference signal with exactly the same frequency and exact phase setting between the signal and the reference. Because of the very narrow bandwidth, the lock-in can make measurements of a small signal that is obscured by random, non-synchronous noise of much greater magnitude. Lock-ins can also give very accurate measurements of signal amplitudes and relative phases between the reference and the signal. The phase and amplitude of the output of the lock-in can be set to refer only to the fundamental frequency of the repetitive signal. Thus, the signals of the excitation light waveform (recorded from the rhodamine sample, which has a very short fluorescence lifetime compared to the fluorescence lifetime of ruby), and of the ruby fluorescence, both recorded with the lock-in, can be thought of as though the excitation signal were a pure sine wave and the fluorescence were a corresponding sine wave at the same frequency. Alternatively, the time-domain signal can be acquired directly in a computer; the time-domain signal can then be analyzed by digital Fourier transform techniques [37] to determine the phase and demodulation (see Footnote 4). In either case, by comparing the phase and relative modulation depth of the fundamental frequency components, we can determine lifetimes according to Eqs. 5 and 6, either at a single frequency, or by carrying out the experiment at several frequencies, and analyzing the frequency dispersion curves of the demodulation or phase.

Examples of time and frequency-domain measurements

Square wave excitation for time and frequency-domain measurements using the rotating light chopper

Sample data are given for both the time-domain and frequency-domain measurement strategies.

Time domain (set-up 1)

Figure 5 shows the exponential decay of the light emitted by the ruby during one half of one cycle (taken at steady state with the equipment in Figs. 1 and 2; see also Fig. 7 for examples of data taken at different repetition frequencies). The data can be averaged over many real-time repetition

cycles with a digital sampling oscilloscope. The data are fitted to one exponential (without deconvoluting the shape of the excitation wave form, which is essentially a square wave at this frequency); the lifetime is 3.7 milliseconds.

Measurement of the sample response relative to a square wave excitation in the frequency-domain and using a lock-in (set-up 2)

The frequency-domain measurement can be carried out in two ways: by determining the amplitude and phase of the output signal for a series of different beam chopper frequencies, or if the lock-in provides the capability, by measuring the amplitude and phase of the higher harmonics of the fundamental frequency. The signal and reference signals are fed into the lock-in amplifier, which is set to display the absolute value of the amplitude and the phase of the signal. The fast-lifetime sample, rhodamine, is used to normalize the phase and modulation depth measurements of the ruby. The phase shift and the depth of the modulation of the ruby sample are then normalized relative to the corresponding values of the rhodamine reference. This is done by subtracting the phase of the ruby signal from the phase of the rhodamine signal, and dividing the modulation depth of the ruby by that of the rhodamine. Because the lifetime of the rhodamine is so short compared to the period of the repetition of the chopped excitation light (six orders of magnitude), the phase and depth of modulation of the rhodamine sample are identical to that of the excitation light. In principle, any compound of known lifetime could be used for this normalization even if the reference lifetime were in the same time range as the sample. Indeed, when measuring nanosecond lifetimes, the reference cannot be considered to be instantaneous compared to the sample; however, if the lifetime of the reference is known, the phase and demodulation of the sample can be calculated. This complication is not necessary with ruby; the rhodamine signal can be considered to represent the wave form of the excitation light. This makes the laboratory exercise with ruby particularly attractive for an introduction to lifetime measurements.

After calibrating the instrument with the rhodamine sample, the ruby sample is placed in the sample holder. Measurements of the amplitude and phase of the signal are then made with the lock-in (Stanford Research Systems, Sunnyvale, Model SR 830 DSP—digital signal processing) for a series of different chopper frequencies, or measuring the higher harmonics of a fundamental repetition frequency (the lock-in we used conveniently does this automatically). The amplitude and phase determinations for each separate frequency give estimations of τ according to Equations 5 and 6. However, it is more accurate to record measurements at several frequencies, rather than just one frequency, and then fit the data by a least squares analysis to the demodulation and phase offset formulae as a function of frequency. If data were acquired at only a single frequency, the estimated lifetimes determined from Equations 5 and 6 would only agree if the actual fluorescence decay is actually a single lifetime component. In addition to being more accurate, multiple lifetimes[3] can be determined from the multiple frequency dispersion curves of the phase and demodulation [2, 4, 6, 38].

Figure 6 shows the fractional modulation and phase data for frequency-domain measurements, taken at many frequencies with a lock-in amplifier (see Fig. 1). The DC excitation light (using an LED) is modulated with the light chopper and the optics and signal amplification of Fig. 3 are used for the measurement. In Figs. 6a and b the frequency of the chopper was varied. In Figs. 6c and d, the chopper is operated at 30 Hz, and the first 5 *odd* harmonics (of the fundamental frequency) were acquired with the lock-in. The even harmonics in the data of Figs. 6c and d do not contain usable data, because the even Fourier components of the signal are negligible. This is easily understood recalling that the even Fourier components of a pure square wave triggering on the rising flank (that is, where the zero time is set to this rising flank) are all zero (see Footnote 2); the rhodamine signal is essentially a square wave at these frequencies, and the even components of the ruby signal are also very small. For the modulation data, Figs. 6a and c, the fits to a single lifetime are quite good, giving $\tau_{\mathrm{mod}} = 3.9$ ms and $\tau_{\mathrm{mod}} = 3.6$ ms. These probably differ because of the different frequency ranges, especially considering that the phase data show a small contribution of a second shorter time. There is a slight deviation of the phase data of Fig. 6b when fit to as a single component. The single lifetime fit shows $\tau_\phi = 3.5$ ms; however, the last three points lie somewhat below the fit (not shown). As expected if there are more than one lifetime component, $\tau_\phi < \tau_{\mathrm{mod}}$, when both sets of data in Figs. a and b are analyzed as a single lifetime at every separate frequency. Therefore, we have fit the phase data of Fig. 6b to two lifetimes. The theory for multi-lifetime fits in the frequency domain is straight forward, but algebraically more involved (see Footnote 3). The fit indicates that 97.5–98% of the frequency domain amplitude is due to a slow component with $\tau_\phi = 3.8$ ms, and the rest to a component faster than the time resolution of our experiments. The phase data of Fig. 6d, which cover a larger frequency range than Fig. 6b, show a very clear contribution of a very fast lifetime component (one component does not

[3] The frequency dependence of each component is described in complex notation by $A_s(i\omega) = A_{s,0}/(1 + i\tau_s\omega)$. If there are S different lifetimes, for every frequency ω_1, the equations corresponding to Equations 5 and 6 are: Modulation $= [(\sum_{s=1}^{s=S} \frac{\alpha_s}{1+(\omega_1\tau_s)^2})^2 + (\sum_{s=1}^{s=S} \frac{(\alpha_s\omega_1\tau_s)}{1+(\omega_1\tau_s)^2})^2]^{1/2}$, and $\Phi_{\mathrm{F},\omega_1} = \tan^{-1}(\sum_{s=1}^{s=S} \frac{(\alpha_s\omega_1\tau_s)}{1+(\omega_1\tau_s)^2} / \sum_{s=1}^{s=S} \frac{\alpha_s}{1+(\omega_1\tau_s)^2})$, where α_i is the fractional amplitude of the ith frequency component at low frequencies, and $\sum_s \alpha_s = 1$.

fit reasonably at all); in this case the two component fit indicates a slow component of $\tau_\phi = 3.7$ ms with 99% of the amplitude.

These data of Fig. 6 demonstrate nicely how the lock-in measures the amplitude and phase of a repetitive signal; in this case, the raw signal is not at all sinusoidal. The lock-in essentially measures the selected Fourier component of the repetitive fluorescence signal, which is detected by the photomultiplier. The amplitude and phase of the selected Fourier component of the signal is calculated by the lock-in through synchronous detection with the repetitive trigger of the chopper. The phase and modulation of the ruby fluorescence (Fig. 6) are then calculated at every frequency relative to an identical measurement with a rhodamine sample. A demonstration of the time course of the signal using the chopper at different frequencies is seen in Fig. 7.

Direct computer data acquisition with Fourier analysis (set-up 2; Fig. 3)

Direct data acquisition with the equipment of Fig. 3 was carried out using either the light chopper with the arc lamp or LED as continuous sources, or modulating the LED directly at different frequencies sinusoidally. The fluorescence was detected with a photomultiplier tube (the PMT is a Hamamatsu, R928). The data were acquired digitally using a National Instruments (Austin) data-acquisition card (PCI-6221; two analog outputs (0–833 kS/s (kilo-samples/sec) output) 16 bit, eight 16-bit analog inputs, 250 kS/s sampling rate). For modulating the LED sinusoidally, we used LabView to generate the analog signal from this National Instrument card. Through this software interface for driving the LED it is easy to create excitation waveforms of white noise, sine waves or any user specified function. The analog output of the National Instrument card can be further amplified depending on the application. The LED, used in some experiments for exciting the sample, is driven by a simple 5 Watt amplifier circuit (ISS, Urbana).

The output current of the PMT is converted to a voltage, amplified, sent through a low pass filter (roll-off of 0.1 milliseconds), and then sent either to a lock-in amplifier or to the analog input of the National Instrument card. If necessary, the data can be averaged over a large number of periods (resulting in an averaged signal over one period). The data are analyzed using digital Fourier transform techniques, to determine the modulation and phase of the signal.[4] Calculating the fundamental frequency (or harmonic) digital transform is equivalent to making a nonlinear regression to a sinusoid [33, 39]. By acquiring the data directly into the computer, the Fourier analysis functions essentially as a digital lock-in.

Using the detection system of Fig. 3a; excitation with the light chopper at different square wave repetition frequencies, and at higher sinusoidal frequencies using the LED in the frequency domain

Using the light chopper

We first consider how to determine fluorescence lifetimes using the chopper in the time and frequency domains, using the equipment of Fig. 3a. Figures 7a,b and c show the fluorescence signals resulting from the approximate square wave excitation derived from the light chopper and acquired directly with the DAC hardware of Fig. 3a.

This method of data acquisition, which is easy to implement with the hardware of Fig. 3a, demonstrates nicely a visual signal (the same would be seen with an oscilloscope). This represents the same signal that was entered into the lock-in amplifier in Fig. 1. Just as the lock-in amplifier selects from this signal the fundamental frequency component (for the rhodamine and ruby samples), the same information can be attained by carrying out a digital Fourier analysis (see Footnote 4) of the digitally acquired signal in Fig. 7. The recorded periods of the time series data using the light chopper can also be fit directly to exponential decays, as explained in our discussion of Fig. 5. We derive a time constant of 3.8 milliseconds for the data in Fig. 7a. For this direct time-domain analysis it is best to choose a repetition frequency that is low enough so that the fluorescence signal of the ruby approximately achieves a plateau (Fig. 7a). In this case, the rise and fall times of the flanks of the excitation light (rhodamine signal) are rapid enough so that a deconvolution with the form of the excitation pulse is not necessary.

Comparing Fig. 7b to Fig. 7a shows the effect of the repetition frequency on the form of the recorded exponential decay. As mentioned previously, the exponential relaxation of the rising signal (light on) is identical to that of the decaying signal (light off). This is always true, even with a very short excitation pulse; however, in that case the two signals are of course not symmetrical. Normally, this feature is not evident, because the light pulse of time-domain nanosecond experiments is very short (100 femtoseconds to a few nanoseconds; in the latter case deconvolution must be

[4] The digital transform of a repetitive function can be calculated easily from the data points in one period, if the points are equally spaced. Call the kth data point D_k. Then form the following summations: $F_{\sin} = \sum_{k=1}^{K} D_k \sin(\theta_k)$, $F_{\cos} = \sum_{k=1}^{K} D_k \cos(\theta_k)$, $\sum_{k=1}^{n} X_i^2$, and $F_0 = 1/K \sum_{k=1}^{K} D_k$; $\theta_k = 2\pi k/K$, and K is the total number of points in one period. The modulation and phase of the fundamental frequency component is the easily calculated. Defining $F_\omega = (F_{\sin}^2 + F_{\cos}^2)^{1/2}$, we have $M_{F,\omega} = F_\omega/F_0$ and $\Phi_\omega = \tan^{-1}(F_{\sin}/F_{\cos})$. This can be extended to higher harmonics.

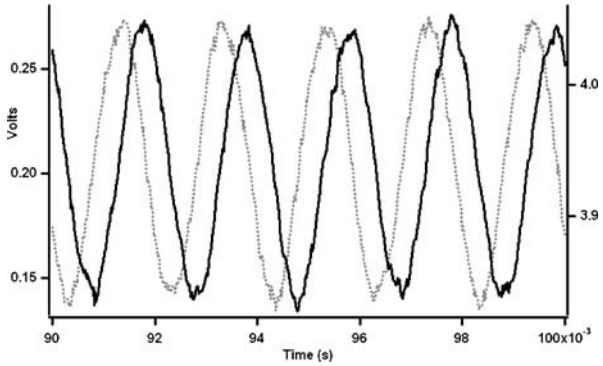

Fig. 8 Rhodamine (dotted grey) and ruby (solid black) emission driven by sine wave modulation at 500 Hz. Left vertical axis is for rhodamine signal, right axis is for ruby. The input and output frequencies are the same, but the modulation and phase differ, as shown in the plot, in which the ruby lags in phase by 84.6 degrees and the ratio of AC/DC components of ruby is 0.0257 compared to 0.316 of rhodamine. The phase and modulation of the rhodamine are affected by instrument response and modulation depth of the LED. Rhodamine is used to correct for instrument response by assuming an instantaneous response to get the true phase and modulation of the ruby

performed). Figure 7c shows the decrease in the modulation as the frequency is increased.

Using sinusoidal modulation

The advantage of using the LED as an excitation source is that higher frequencies of excitation can be achieved easily, and we can apply any desired waveform of excitation (the form of the excitation waveform is calculated by the computer program). In this case, using sinusoidal modulation, higher frequencies can be analyzed. Figure 8 shows a time series recording applying a sinusoidal driving signal to the LED, using the data acquisition system of Fig. 3a.

The reduction in the modulation and the phase lag of the ruby fluorescence compared to the rhodamine sample is clearly seen in this time series acquisition (which can also be displayed on a simple oscilloscope). The modulation depth and phase of the recordings are analyzed with a Fourier analysis of the digitally recorded data. Figures 9a and b show plots of the modulation and phase of the ruby (where the modulation level and the phase of the ruby sample are relative to the corresponding parameters of the rhodamine signal).

As with the lock-in data we find that we can fit the modulation data with a single lifetime component. The single component of the modulation has $\tau_{\mathrm{mod}} = 3.9$ ms. However, the phase data show large deviations from a single component at higher frequencies. To fully analyze this data one has to include more than one lifetime, as described in Footnote 3. The two component analysis of the phase data has $\tau_{\phi} = 3.3$ ms with greater than 99% of the amplitude corresponding to this time constant. The lifetime of the faster component is again too short to be analyzed with our frequency response, but the amplitude is assessable, and the effect on the phase is clearly revealed. Fitting routines of two components are easy to write, and can be written in any available computer analysis software. Further discussion of this is beyond the purpose of this report; however, it is a good exercise for the students. It is easy to see why the phase will decrease at higher frequencies even if the very fast component makes a minor contribution to the intensity of fluorescence. When the frequency becomes so high that the modulation (dynamic amplitude) of the 3.7–3.9 ms component becomes negligible, higher frequency components will contribute relatively much more to the detected signal. The phase delay of the detected signals at higher frequencies derived from the longer lifetime component becomes negligible, and the phase at these higher frequencies will eventually decrease to that corresponding to that of the very fast component alone. Because the modulation of the slow component has already decreased drastically at the higher frequencies, the very small contribution of the faster component is not seen in the modulation data. The ability of the phase data to reveal a very small faster fluorescence component (also in the nanosecond measurements) is one of the advantages of the frequency-domain. However, this component could also be due to a small leakage of the excitation light to the detector. The lifetime from the fit of the phase data is shorter than all the other determinations in this paper. This is probably because we only have seven frequencies, and the double component analysis involves three fitted parameters. In addition, the contribution of the higher frequency component is extremely small, in spite of the fact that this faster component dominates the high frequency signal, which in this case extends to 2000 Hz. The modulation data are fit with fewer parameters, and the defining component extending through the amplitude data is the single, major 3.7 ms component.

Spectrum analysis and audio demonstration

A perspicuous demonstration comparing the frequency dispersion of the fluorescence signal from rhodamine and ruby can be performed by modulating the excitation light with a wide spectrum of frequencies. A good qualitative feel for the decreasing amplitude of the ruby luminescence response can be gained by the following measurements.

As noted for the frequency-domain lifetime measurement, the amplitude of the output signal is demodulated (the depth of modulation decreases) as the modulation frequency is increased. If the LED is modulated by an audio frequency input (the frequencies corresponding to the ruby lifetime are conveniently in the audio range) the output signal will be demodulated increasingly at the higher frequencies. An approximate incoherent white noise input, which has a very

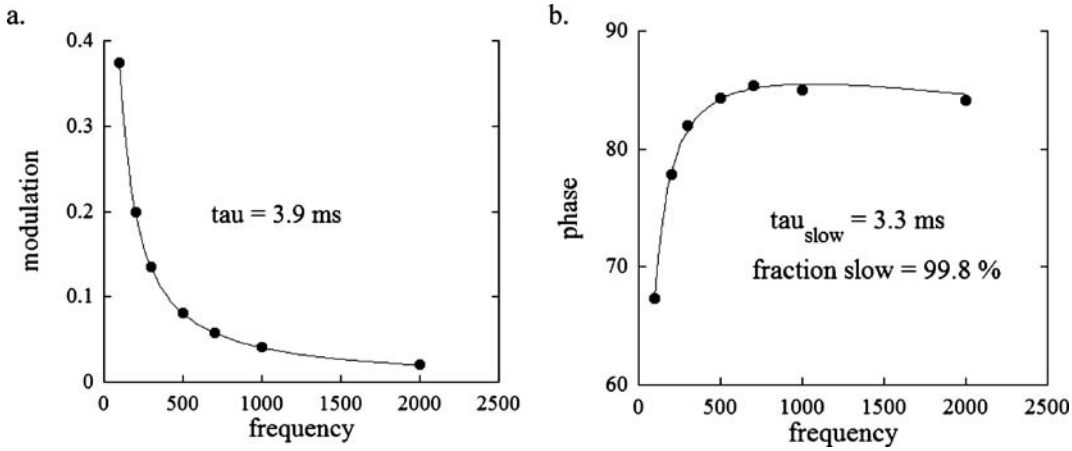

Fig. 9 Modulation, a), and phase, b), vs. frequency of the experiment carried out with the sinusoidally modulated LED light. The data in a are fit to the expression for modulation of a single component, Equation 5. The phase data of b are fit to an expression for two components, see Footnote 3. See the text for the explanation why we cannot observe the minor, very fast second component in the modulation. Note, although the minor component is less that 1%, at the higher frequencies it is easily seen in the phase data

broad frequency spectrum in the frequency range of interest, see Figs. 3a, 10 and 11a, can be applied to the LED from the DAC of the computer. The frequency components of the applied "white noise" are not synchronized in phase. Because the fluorescence decay of ruby is conveniently in the frequency spectrum of normal audio signals with a broad frequency spectrum, the driving signal can also be derived from music (Figs. 3b and 13). The demodulation of the fluorescence signal from ruby at higher frequencies is equivalent to sending the audio signal (white noise or music) derived from the fluorescence light through a low frequency filter; the filter in this case is not an electronic filter, but the long lifetime of the ruby fluorescence.

White noise modulation

A time recording of the fluorescence data from the white noise input (Fig. 10) over a longer time can be acquired directly with our DAQ card with a high time resolution.

The different frequency responses of the rhodamine and ruby samples are clearly seen in the raw data of the time series experiment (Fig. 10). The higher frequency components are clearly reduced for the ruby compared to rhodamine. This can be quantified by carrying out a Fast Fourier Transform of the signal. From this analysis of the signals the power spectrum[5] of the ruby signal can be seen to decrease significantly at higher frequencies relative to that of the frequency spectrum of the rhodamine (Fig. 11a–c). The reduction of the high frequency components of the rhodamine signal is due to a $\sim$0.1 ms time constant of the current-to-voltage amplifier between the PM and the computer input. Otherwise the rhodamine signal frequency components would track that of the input white noise.

In Fig. 12a the power spectrum of the ruby is normalized by the power spectrum of the rhodamine and the amplitude (amplitude $= \sqrt{\text{power}}$) is plotted on a linear frequency scale. The lifetime can be extracted by fitting this data to the expression in the figure legend of Fig. 12. The result is $\tau = 3.7$ ms.

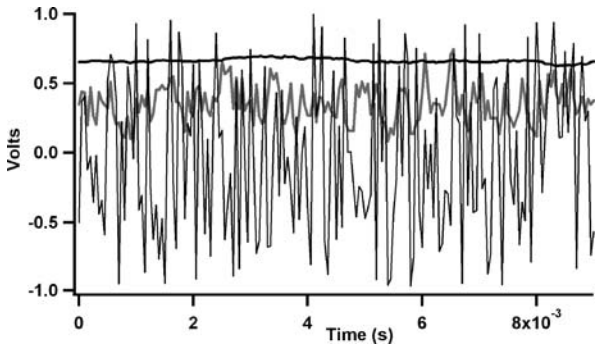

Fig. 10 White noise modulation of the diode. Displayed is the white noise output (thin black) sent directly into an analog input. Thick grey is the signal as recorded by the PMT through rhodamine fluorescence and thick black is the signal from ruby, which has only a slight modulation when viewed on this short a timescale and displays mostly low frequency components as compared to the rhodamine and analog output of the DAQ card. The current to voltage converter from the PMT contains a 2 kHz (0.16 msec) roll-off, thus the signal from rhodamine also appears as a low pass filter due to the electronics, yet rolls of at much higher frequency. The ouput of rhodamine and ruby are both positive because analog output which modulates the LED is superimposed on a DC offset and modulation depth of the LED is less than or equal to 100%

[5] The power spectrum of a repetitive signal is related to the squares of the Fourier coefficients. Let the Fourier decomposition of the time dependent signal be $y(t) = A_0/2 + \sum_{m=1}^{\infty} (A_m \cos m\omega_0 t + B_m \sin m\omega_0 t)$; see Footnote 1. The total power in the mth component is then defined as $P_y(m\omega_0) = 1/2(A_m^2 + B_m^2)$. The last expression plotted versus $\log(m\omega_0)$ constitutes the power spectrum.

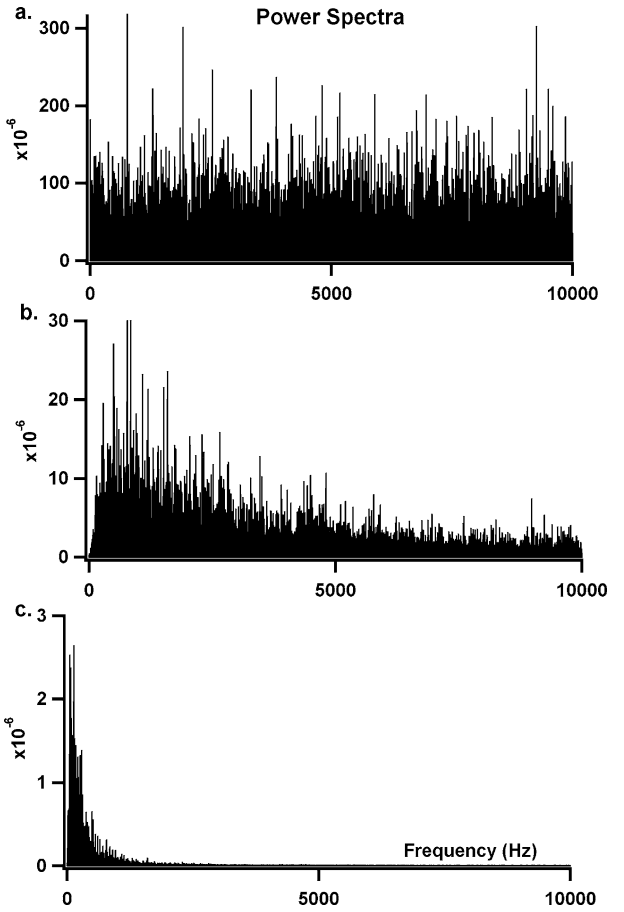

Fig. 11 Power spectra (see Footnote 1) of the data in Fig. 7: a) analog output, b) signal through the rhodamine and c) signal through the ruby. The 2 kHz roll-off is clearly seen from the rhodamine data,. The ruby data have a much more dramatic roll-off at lower frequencies. The dramatic decreasing amplitude of the modulation of the ruby fluorescence with increasing frequency is due to the long fluorescence lifetime of ruby

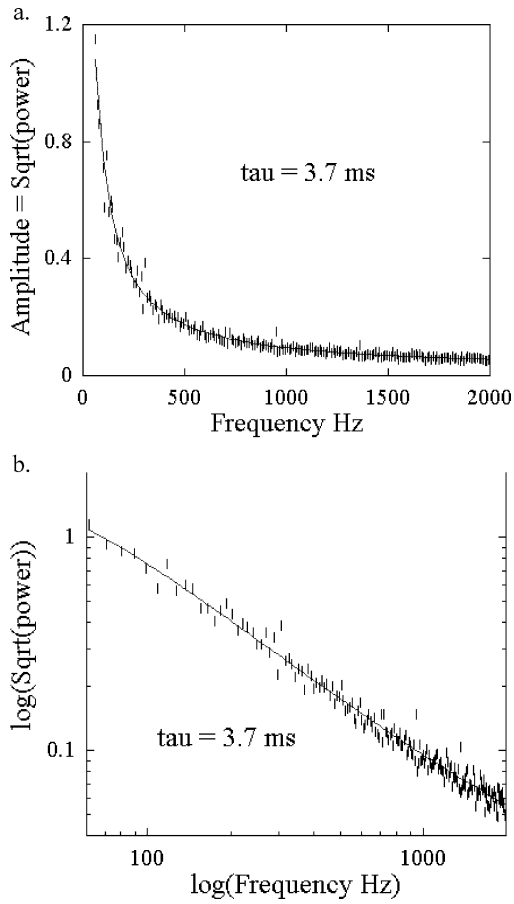

Fig. 12 (a).The $\sqrt{\text{(power spectrum ruby)/(power spectrum rhodamine)}}$ is plotted versus the frequency in Hz, open circles. This ratio is fit to the expression, $A(\omega) = A_0/\sqrt{1+(2\pi f\tau)^2}$, solid line, see text. The lifetime from this fit is 3.7 ms. Because the power spectrum of rhodamine is taken separately from that of ruby, A_0 is not one, and is included as a parameter in the fitting. There are also other contributions to the noise (eg from the photomultiplier), and this is taken into account in the fit by including the addition of a constant plateau. Because the output of the noise was created on a linear frequency scale, i.e. not flat on a logarithmic scale, it was necessary to bin the power spectra by $\sim$10 Hz intervals due to low statistics at low frequency. The white noise measurement is not synchronized to the phase of the excitation modulation, so there is no information on phase. (b) The $\log[\sqrt{\text{(power spectrum ruby)/(power spectrum rhodamine)}}]$, vertical lines, is plotted versus $\log(f,\text{Hz})$. Note that we have normalized the power spectrum of ruby has been normalized by the rhodamine signal of Fig. 11b. This is identical to a Bode plot (see text), except we have not multiplied by 20 so it is not in dB units. A simulation of $\log(1/\sqrt{1+(2\pi f\tau)^2})$ is also plotted, with $\tau = 3.7$ ms, solid line

In Fig. 12b a plot of the data and fit is shown in a form similar to a Bode Plot in the electronics literature. The time response of the ruby decay can be derived from the 3 dB point of this plot; however, we have analyzed the data from Fig. 12a to derive the lifetime. The Bode plot for electronic amplifiers is derived from the response of the amplification with frequency, which is defined in the frequency domain by expressing the frequency dependence of the amplification in complex notation as $A(i\omega) = A_0/(1+i\tau\omega)$. In the time domain this is an exponential decay. τ is the exponential time constant of the high frequency roll-off filter (assuming only a simple one time constant high frequency filter), $i = \sqrt{-1}$, and A_0 is the low frequency amplification [40]. This is the same expression defining the frequency response of a single lifetime of fluorescence in the frequency domain (see Footnote 3) [4]; however, in the fluorescence lifetime measurement we measure the roll-off of the modulated fluorescence signal as the frequency increases. In the electronics literature, the magnitude in decibels is defined as $|A(\text{dB})| \equiv 20\log|A| = 20\log|A_0| - 20\log(\sqrt{1+(\omega\tau)^2})$. In the usual case of frequency domain fluorescence lifetime measurements, the demodulation is normalized so that $A_0 = 1$ (Equation 5). When the excitation consists of white noise, we have no phase information, but the amplitude of the frequency response is just the modulation (the real amplitude) of the complex

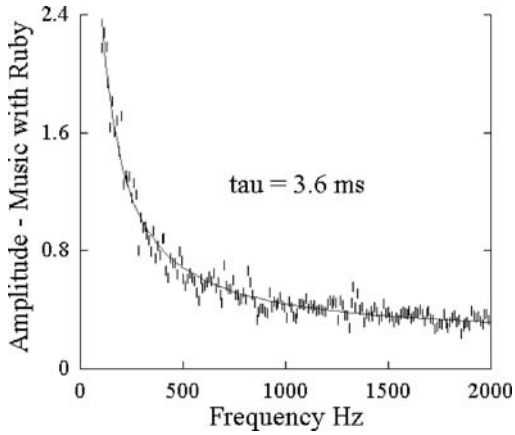

Fig. 13 Amplitude spectrum of the emission of ruby in response to the excitation light that is modulated by an audio signal (music). The sampling is 44100 Hz/16 bit. The frequency response of the ruby has been corrected (divided by) the frequency response of rhodamine (as in Fig. 12). The result of the FFT was binned by 1000 to reduce amount of data points in graph. The frequency response/content of our system is limited to frequencies below 10 kHz; however, we only show the frequencies of interest for the demodulation by the ruby emission. The low pass property of the Ruby is reflected in the decrease in the response to higher frequencies, and the lifetime agrees well with the other determinations

number $A(i\omega) = A_0/(1 + i\tau\omega)$, the same as for the electronic filter. The Bode plot is defined as $20\ \log(A/A_0) = -|A/A_0|$dB versus $\log(\omega\tau)$. The lifetime can then be determined from the 3 dB point ($3 = 20\ \log(\sqrt{2})$), which is the point where $\omega_{3\text{dB}} = 1/\tau$, where $|A/A_0|$ has decreased to 0.707 of its original value. When we are dealing with power, then: $\left|A^2(\text{dB})\right| \equiv 10\ \log|A^2| = 10\ \log|A_0^2| - 10\ \log(1 + (\omega\tau)^2)$. The power is proportional to the complex conjugate squared of the amplitude $|A(i\omega)^2| = [A_0/(1 + i\tau\omega)][A_0/(1 - i\tau\omega)]$. The real amplitude is therefore the square root of the power spectrum. By fitting the square root of the power spectrum to the same function representing the modulation described in Equation 5 the lifetime can be determined. In the fit (see Fig. 12a) we must include an arbitrary amplitude, because we do not have a direct measure of the low frequency limit of the ruby data. This is because the division of the ruby power spectrum data by the rhodamine power spectrum data results in an arbitrary amplitude (the two measurements are taken with different instrumentation amplification). In Fig. 12b we have plotted the data of Fig. 12a; thus, Fig. 12b is the Bode plot representation. The lifetime would be found from this plot at the point on the frequency axis where the amplitude is reduced to 0.707 of the low frequency value, or where the power is reduced to 0.5 of its low frequency value. The 3 dB point of the Bode plot in Fig. 12 is difficult to determine visually because of the noise and the few points at these frequencies; however, one can see that it lies in the expected frequency range. In addition, we do not have data at the very low frequencies; but the plot shows nicely the goodness of the fit throughout the entire frequency range, which is not so evident from the plot in Fig. 12a. The white noise method is only rarely used for determining luminescence lifetimes. Direct time- or synchronous frequency-domain data acquisition (Figs. 5–9) are much more common. This is due to the unavailability of a white noise light source, and the inability to reduce the noise frequency bandwidth, which is the hallmark of synchronous detection in the frequency domain. However, this is an excellent exercise for the students to realize the correspondence between fluorescence lifetime measurements and measurements that are ubiquitous in the electronics literature [41].

Lifetime music

The output of the photomultiplier can also be amplified, and sent through a power amplifier to an audio system (Fig. 3b). This can be an amplifier from a stereo system; we used an Optimus MPA-125 100 W audio amplifier connected to loudspeakers (16 ohm, 5 W). A smaller amplifier whose output power matches that of the speakers is preferred; otherwise, there is a risk of damaging the speakers. We used this amplifier only for convenience. For these experiments, the audio output of the computer playing a MP3 music file is sent through a 5 W power amplifier that is driving the LED, as above. The current of the photomultiplier is converted to a voltage, passed through a high pass filter (to reduce the DC offset, and very low frequencies), sent through an audio amplifier into the speakers. Alternatively the output form the PMT can be collected into the PC by a sound-card with any convenient music recording system (Audiograbber). The data can also be collected with the DAQ card with LabView, and later converted to a ".wav" file, which can then be played on the audio output of the computer system.

If the input modulation of the LED is from music with a broad bandwidth and the right frequency spectrum, the high frequency components of the music will be damped by the slow response time of the ruby, but not by the rhodamine sample. Listening to sound clips with high and low frequency components through both the ruby and rhodamine samples can give the students a good qualitative understanding of the lifetime differences. The basic physics behind the measurement is clearly heard, and the experiment is fun and enjoyable for the students. With a little practice one can "hear" the value of the lifetime. The lifetime of the ruby can be varied by changing the temperature of the sample holder [18]. The data acquired with the computer with a music recording system are analyzed the same as the white noise data of Fig. 12. The plot (Fig. 13) of the frequency spectrum clearly shows the decrease in the amplitude spectrum at higher frequencies for the ruby sample, and the fitted lifetime, 3.6 ms, is identical to the other lifetime determinations. Listening to music

with a large amount of bass and also high amount of treble, the demodulation of the high frequency components can be easily discerned.

Summary

By using a convenient sample (ruby) with a long lifetime (approximately 3 milliseconds) instructive demonstrations of the time- and frequency-domain methods of fluorescence lifetime determinations can be carried out. The required instrumentation is minimal, and is within the reach of most teaching laboratories. The data analysis can be written by the laboratory participants with any available data analysis software or spread sheet, acquainting the students with the physics and mathematical background of the different methods of measurement. The students can also assemble much of the instrumentation. We have found these hands-on experiments to be highly instructive. The participants acquire a better understanding of experimental procedures that are also applicable to nanosecond measurements using much more sophisticated instrumentation.

Acknowlgments We thank the students of the Physics 590OS optical spectroscopy class for their enthusiastic participation, Ulai Noomnarm and Chittanon Buranachai for reading the manuscript and giving feedback, Jack Bopari, the director of the undergraduate teaching laboratories in the Physics department, for his generosity loaning equipment and the ruby sample, Eugene Colla for assistance assembling Setup 1 for partial fulfillment of the senior thesis project of DEC, and RMC thanks Gerard Marriott for his enjoyable participation years ago when the idea of listening to phosphorescence lifetimes was born.

References

1. Cubedda R, Comelli D, D'Andrea C, Taroni P, Valenti G (2002) Time resolved fluorescence imaging in biology and medicine. J Phy D: Appl Phy 35:R61–R76
2. Schneider P, Clegg R (1997) Rapid acquisition, analysis, and display of fluorescence lifetime-resolved images for real-time applications. Rev Sci Instrum 68(11):4107–4119
3. Redford GI, Clegg RM (2005) In: Periasamy A, Day RN (eds) Molecular Imaging: FRET Microscopy and Spectroscopy. Oxford University Press, New York, pp 193–226
4. Clegg RM, Schneider PC (1996) In: Slavik J (ed) Fluorescence Microscopy and Fluorescent Probes. Plenum Press, New York, pp 15–33
5. Clegg RM, Holub O, Gohlke C (2003) Fluorescence lifetime-resolved imaging: measuring lifetimes in an image. Methods Enzymol 360:509–542
6. Gratton E, Jameson DM, Hall R (1984) Multifrequency phase and modulation fluorometry. Ann Rev Biophys Bioeng 13:105–124
7. Goldman S (1948) Frequency analysis, modulation, and noise. Dover, New York
8. Willison JR (1985) Lock-in amplifiers and measurement techniques. Lasers and Applications March, 73–76
9. Hieftje GM (1972) Signal-to-noise enhancement through instrumental techniques. Part I. Signals, noise, and S/N enhancement in the frequency domain. Anal Chem 44(6):81A–88A
10. Hieftje GM (1972) Signal-to-noise enhancement through instrumental techniques. Part II. Signal averaging, boxcar integration, and correlation techniques. Anal Chem 44(7):69A–78A
11. Billington C (1960) Phosphorescence mechanisms. I. Approach and general analysis. Phys Rev 120(3):697–701
12. Billington C (1960) Phosphorescence mechanisms. II. Description of phosphorometer. Phys Rev 120(3):702
13. Billington C (1960) Phosphorescence mechanisms. III. Method of analysis. Phys Rev 120(3):708–709
14. Billington C (1960) Phosphorescence mechanisms. IV. Decay rate spectrum of ruby, uranium glass, and mn-activated zinc sulfide. Phys Rev 120(3):710-714
15. Aizawa H, Uchiyama H, Katsumata T, Komuro S, Morikawa T, Ishizawa H, Toba E (2004) Fibre-optic thermometer using sensor materials with long fluorescence lifetime. Meas Sci Technol 15:1484–1489
16. Temple PA (1975) An introduction to phase sensitive amplifiers: An inexpensive student instrument. Am J Phys 43(9):801–807
17. Scofield JH (1994) Frequency-domain description of a lock-in amplifier. Am J Physics 62(2):129–133
18. Alcala JR, Liao S-C, Zheng J (1996) Real time frequency domain fiberoptic temperature sensor using ruby crystals. Mod Eng Phys 18(1):51–56
19. Birks JB (1970) Photophysics of aromatic molecules. Wiley, London
20. Parker CA (1968) Photoluminescence of solutions. Elsevier, Amsterdam
21. Cherry RJ (1979) Rotational and lateral diffusion of membrane proteins. Biochim Biophys Acta 559:289–327
22. Zidovetzki R, Yarden Y, Schlessinger J, Jovin TM (1981) Rotational diffusion of epidermal growth factor complexed to cell surface receptors reflects rapid microaggregation and endocytosis of occupied receptors. Proc Natl Acad Sci USA 6981–6985
23. Vanderkooi JM, Maniara G, Green TJ, Wilson DF (1987) An optical method for measurement of dioxygen concentration based upon quenching of phosphorescence. J Biol Chem 262(12):5476–5482
24. Mik EG, Donkersloot C, Raat NJH, Ince C (2002) Excitation pulse deconvolution in luminescence lifetime analysis for oxygen measurements in vivo. Photochem Photobiol 76(1):12–21
25. Holst G, Kohls O, Klimant I, Koenig B, Kuehl M, Richter T (1998) A modular luminescence lifetime imaging system for mapping oxygen distribution in biological samples. Sensors Actuators B 51:163–170
26. Bell JH, Schairer ET, Hand LA, Mehta RD (2001) Surface pressure measurements using luminescent coatings. Annu Rev Fluid Mech 33:155–206
27. Parker D, Senanayake PK, Williams JAG (1998) Luminescent sensors for pH, pO2, halide and hydroxide ions using phenanthridine as a photosensitiser in macrocyclic europium and terbium complexes. J Chem Soc Perkin Trans 2:2129–2139
28. Marriott G, Clegg R, Arndt-Jovin D, Jovin T (1991) Time resolved imaging microscopy. Biophys J 60:1374–1387
29. Selvin P, Hearst J (1994) Luminescence energy transfer using a terbium chelate: Improvements on fluorescence energy transfer. Proc Natl Acad Sci USA (91):10024–10028
30. Silfvast WT (1996) Laser fundamentals. Cambridge University Press, New York
31. Davis CC (1996) Lasers and electro-optics: Fundamentals and engineering. Cambridge University Press, Cambridge
32. Butz T (2006) Fourier transformation for pedestrians. Springer-Verlag, Berlin
33. Bracewell RN (1965) The Fourier transform and its applications, 2nd ed, McGraw-Hill, Kogakusha Ltd., Tokyo

34. Hamming RWH (1989) Digital filters, 3rd ed, Dover Publications, Inc., Mineola
35. Dern H, Walsh JB (1963) In: Nastuk WL (ed) Physical techniques in biological research; Electrophysiological methods Part B. Academic Press, New York, pp 99–217
36. Wolfson R (1991) The lock-in amplifier: A student experiment. Am J Phys 59(6):569–572
37. Brigham EO (1988) The fast Fourier transform and its applications. Prentice Hall, Englewood Cliffs
38. Lakowicz JR (1999) Principles of fluorescence spectroscopy, 2nd ed, Kluwer Academic, New York
39. Hamming RWH (1973) Numerical methods for scientists and engineers. Dover Publications, Inc., New York
40. Millman J, Halkias CC (1972) Integrated Electronics: Analog and digital circuits aqnd systems, 1st ed, McGraw-Hill Book Company, New Your
41. Delaney CFG (1969) Electronics for the physicist. Penguin Books Inc., Baltimore